JOC Article

Deprotonation Sites of Acetohydroxamic Acid Isomers. A Theoretical and Experimental Study

María L. Senent,[†] Alfonso Niño,[‡] Camelia Muñoz Caro,[‡] Satunino Ibeas,[§] Begoña García,*[,§] José M. Leal,[§] Fernando Secco,[||] and Marcella Venturini[||]

Departamento de Astrofísica Molecular e Infrarroja, Serrano 113b, Madrid 28006, Spain, Grupo de Química Computacional, Escuela Superior de Informática, Universidad de Castilla la Mancha, Paseo de la Universidad, 4, 13071 Ciudad Real, Spain, Departamento de Química, Universidad de Burgos, Misael Bañuelos s/n, 09001 Burgos, Spain, and Dipartimento di Chimica e Chimica Industriale, Università di Pisa, Via Risorgimento 35, 56126 Pisa, Italy

begar@ubu.es

Received February 4, 2003

Theoretical (ab initio calculations) and experimental (NMR, spectrophotometric, and potentiometric measurements) investigations of the isomers of acetohydroxamic acid (AHA) and their deprotonation processes have been performed. Calculations with the Gaussian 98 package, refined at the MP2-(FC)/AUG-cc-pVDZ level considering the molecule isolated, indicate that the *Z*(cis) amide is the most stable form of the neutral molecule. This species and the less stable (*Z*)-imide form undergo deprotonation, giving rise to two stable anions. Upon deprotonation, the *E*(trans) forms give three stable anions. The ab initio calculations were performed in solution as well, regarding water as a continuous dielectric; on the basis of the relative energies of the most stable anion and neutral forms, calculated with MP2/PCM/AUG-cc-pVDZ, N-deprotonation of the amide (*Z* or *E*) structure appeared to be the most likely process in solution. NMR measurements provided evidence for the existence of (*Z*)- and (*E*)-isomers of both the neutral and anion forms in solution. Comparisons of the dynamic NMR and NOESY (one-dimensional) results obtained for the neutral species and their anions were consistent with N-deprotonation, which occurred preferentially to O-deprotonation. The (microscopic) acid dissociation constants of the two isomers determined at 25 °C from the pH dependence of the relevant chemical shifts, $pK_E = 9.01$ and $pK_Z = 9.35$, were consistent with the spectrophotometric and potentiometric evaluations ($pK_{HA} = 9.31$).

Introduction

Hydroxamic acids are very useful reagents with interesting biological activity and medical applications. Due to their ability to form stable chelates with a variety of metal ions, hydroxamic acids play a key role as bioligands in the microbial transport of iron (siderophores); the ease in forming metal chelates facilitates the function of enzymes in oxygen and electron transport and in other life-sustaining processes.[1] Despite their interesting properties, hydroxamic acids have remained as a poorly characterized class of organic compounds; assignment of the correct structure has been a major difficulty because these compounds may adopt several forms.[2] Knowledge of the preferred ionization sites and the protonation−deprotonation mechanism is essential to learning the role played by hydroxamic acids in biological and complexation processes.

Previously, we investigated acetohydroxamic acid using experimental and theoretical tools.[3,4] At high acidity levels, the neutral AHA molecule can accept one proton. The stable cations and neutral AHA forms have been studied with ab initio methods of good quality;[3,4] calculations predict bonding of the proton to the hydroxylamine oxygen group, which produces a third stable cation in the presence of solvent, the CO oxygen being the most basic site. Calculations in the gas phase suggest different amidic and imidic structures that become stabilized by intramolecular H-bonds.[3,4]

The most stable AHA forms in the solid state were found to be those prone to intermolecular H-bonding;[5] *Z*−*E* isomerism was observed for AHA in DMSO[6] and for monoalkylhydroxamic acids in several solvents.[7] On the basis of theoretical calculations and comparative data

[†] Departamento de Astrofísica Molecular e Infrarroja.
[‡] Universidad de Castilla la Mancha.
[§] Universidad de Burgos.
[||] Università di Pisa.

(1) Brown, D. A.; Chidambaram, M. V. In *Metal Ions in Biological Systems*; Marcel Dekker: New York, 1982; Vol. 14.
(2) Bauer, L.; Exner, O. *Angew. Chem., Int. Ed. Engl.* **1974**, *13*, 376. Ventura, O. N.; Rama, J. B.; Turi, L.; Dannenberg, J. J. *J. Am. Chem. Soc.* **1993**, *115*, 5, 5754. Ventura, O. N.; Rama, J. B.; Turi, L.; Dannenberg, J. J. *J. Phys. Chem.* **1995**, *99*, 131.
(3) Muñoz-Caro, C.; Niño, A.; Senent, M. L.; Ibeas, S.; Leal, J. M. *J. Org. Chem.* **2000**, *65*, 405.
(4) García, B.; Ibeas, S.; Leal, J. M.; Senent, M. L.; Niño, A.; Muñoz-Caro, C. *Chem-Eur. J.* **2000**, *6*, 2644.
(5) Lindberg, B.; Berndtsson, A.; Nilsson, R.; Nyholm, R.; Exner, O. *Acta Chem. Scand.* **1978**, *A32*, 353.
(6) Brown, D. A.; Glass, W. K.; Mageswaran, R.; Girmany, B. *Magn. Reson. Chem.* **1988**, *26*, 970.
(7) (a) Brown, D. A.; Glass, W. K.; Mageswaran, R.; Mohammed, S. A. *Magn. Reson. Chem.* **1991**, *29*, 40. (b) Brown D. A.; Cufle, L. P.; Fitzpatrick, G. M.; Fitzpatrick, N. J.; Glass, W. K.; Herlihy, K. M. *Collect. Czech. Commun* **2001**, *66*, 99.

10.1021/jo0341564 CCC: $25.00 © 2003 American Chemical Society
Published on Web 07/18/2003

obtained with amides,[8] it has been reported that the *Z*(cis) conformation of monohydroxamate group (CONHOH) is preferentially stabilized by intramolecular H-bonding in nonpolar solvents[9] or by H-bonding in water.[10] NMR and UV studies performed on the structure and acid−base behavior, respectively, of *N*-phenylbenzohydroxamic acid have shown that the Z(cis):*E*(trans) ratio strongly depends on the solvent used.[11] A property that has been paid some attention but is the origin for certain controversy is the acid−base behavior of hydroxamic acids. O- versus N-deprotonation has received different interpretations. First, it was accepted that hydroxamic acids are O-acids,[6,12−14] but extensive IR and UV measurements in dioxane and aqueous alcohol[15] indicate that hydroxamic acids are N-acids, a conclusion supported by ^{17}O NMR and FT-IRC studies of benzohydroxamate ion in MeOH.[12,16] Potentiometric measurements compatible with O- and N-deprotonation of hydroxamic acids have been reported[2,17−19] assuming that the acid dissociation constant $K_{exp} \approx K_{OMe} + K_{NMe}$; however, irregularities attributed to solvent effects have been observed.[2,14b,19,20]

The most probable deprotonation processes of AHA were also investigated with ab initio methods. Previous ab initio calculations of the isolated molecules confirm the NH-acidity on the basis of the anions relative energies.[21−23] Most of the ab initio studies on acid−base properties of hydroxamic acids concern formoacetohydroxamic acid, which appears to dissociate most probably by N-deprotonation.[24−27] To get additional insight into the deprotonation sites of AHA, this work undertakes a theoretical and experimental study of this acid at different temperatures; the solvent effect was included considering water as a continuous dielectric. Relevant NMR information on the deprotonation process and on conformational isomerism is compared with the thermodynamic results. The microscopic constants determined by NMR are consistent with the macroscopic value obtained from potentiometric and UV−vis measurements.

Computational Details

The ORIGIN 3800 IRIX 64 processor computer of the CTI of C.S.I.C. (Madrid) was used for computation. All ab initio calculations were performed with the Gaussian 98 (Revision A.1x)[28] program at the MP2/AUG-cc-pVDZ level. Original Fortran codes have been designed for the treatment of the data. The zero-point vibrational energy and thermodynamic properties of the species in the gas phase have been calculated at the MP2/AUG-cc-pVDZ level using the harmonic approximation and the rigid rotor approximation for all the conformers.

In the calculations performed in solution, water was regarded as a continuous dielectric, characterized by a constant permittivity. The Polarized Continuum Model (PCM) was used, implemented in the Gaussian 98 package[29] using the same basis at the MP2 level. The cavity radii are those recommended for the UAHF model.[29] The solvent dielectric constant has been set at 78.5 for $T = 298.15$ K, 74.8 for $T = 308.15$ K, and 71.5 for $T = 318.15$ K.[30] The changes of free energy in solution have been computed according to the recipes given in ref 31.

Results and Discussion

Theoretical Results: Neutral Forms. The starting species for the quantum mechanical analysis were the neutral stable structures already described (Figure 1), which were found with the MP2/cc-pVDZ method and full geometry optimization.[3] The calculations performed with the Gaussian 98 package were refined using the AUG-cc-pVDZ basis set, which is more appropriate for the treatment of anion species.[28,32] Searching for the stable anions and simulation of the chemical dissociation processes were performed starting from the reoptimized neutral structures.

(8) (a) Hupe, D. J.; Wu, D. *J. Am. Chem. Soc* **1977**, *99*, 7653. (b) Yamaki, R. T.; Paniago, E. B.; Carvalho, S.; Howarth, O. W.; Kam, W. *J. Chem. Soc., Dalton Trans*. **1977**, *24*, 4817. (c) Keeffe, J. R.; Jencks, W. P. *J. Am. Chem. Soc.* **1983**, *105*, 265.
(9) Liczynska-Kochany E.; Iwamura, H. *J. Org. Chem*. **1982**, *47*, 5277.
(10) Brown, D. A.; Coogan, R. A.; Fitzpatrick, N. J.; Glass, W. K.; Abukshima, D. A.; Shiels, L.; Ahlgrén, M.; Smolander, K.; Pakkanen, T. T.; Peräkylä, M. *J. Chem. Soc., Perkin Trans. II* **1996**, 2673.
(11) García, B.; Ibeas, S.; Muñoz, A.; Leal, J. M.; Ghinami, C.; Secco, F.; Venturini, M. *Inorg. Chem*. 2003, in press.
(12) Palm, V. A., Ed. *Tables of Rate and Equilibrium Constants of Heterocyclic Organic Reactions*; VINITI: Moscow, 1975.
(13) Monzky, B.; Crumbliss, A. L. *J. Org. Chem*. **1980**, *45*, 4670.
(14) (a) Bagno, A.; Comuzzi, C.; Scorrano, G. *J. Am. Chem. Soc.* **1994**, *116*, 916. (b) Bagno, A.; Scorrrano, G. *J. Phys. Chem*. **1996**, *100*, 1536.
(15) Exner O.; Kakác, B. *Collect. Czech. Chem. Commun*. **1963**, *28*, 1656.
(16) Exner, O.; Holubek, J. *Collect. Czech. Chem. Commun*. **1965**, *30*, 940.
(17) (a) Bordwell, F. G.; Fried, H. E.; Hughes, D. L.; Lynch, T. S.; Satish, A. V.; Whang, Y. E. *J. Org. Chem*. **1990**, *55*, 3330. (b) Bordwell, F. G.; Liu, W. Z. *J. Am. Chem. Soc.* **1996**, *118*, 8777.
(18) Decouzon M.; Exner, O.; Gal, J. F.; Maria P. C. *J. Org. Chem*. **1990**, *55*, 3980.
(19) Exner, O.; Hradil, M.; Mollin, J. *Collect. Czech. Chem. Commun*. **1993**, *58*, 1109.
(20) (a) Monzky, B.; Crumbliss, A. L. *J. Org. Chem*. **1980**, *45*, 4670. (b) Brink, C. P.; Crumbliss, A. L. *J. Org. Chem*. **1982**, *47*, 1171. (c) Brink, C. P.; Fish, L. L..; Crumbliss, A. L. *J. Org. Chem*. **1985**, *50*, 2277.
(21) Ventura, O. N.; Rama, J. B.; Turi, L.; Dannenberg, J. J. *J. Am. Chem. Soc.* **1993**, *115*, 5754.
(22) Yamin, L. J.; Ponce, C. A.; Estrada, M. R.; Vert, F. Tomas *J. Mol. Struct. (THEOCHEM)* **1996**, *360*, 109.
(23) Remko, M. *J. Phys. Chem. A* **2002**, *106*, 5005.
(24) Remko, M.; Mach, P.; Scheleyer, P. R.; Exner, O. *J. Mol. Struct. (THEOCHEM)* **1993**, *279*, 139.
(25) Stinchcomb, D. M.; Pranata, J. *J. Mol. Struct. (THEOCHEM)* **1996**, *370*, 25.
(26) Remko, M. *Phys. Chem. Chem. Phys.* **2000**, *2*, 1113.
(27) Yen, S. J.; Lin, C. Y.; Ho, J. J. *J. Phys. Chem. A* **2000**, *104*, 11771.
(28) Frisch, M. J.; Trucks, G. W.; Schlegel, H. B.; Scuseria, G. E.; Robb, M. A.; Cheeseman, J. R.; Zakrzewski, V. G.; Montgomery, J. A., Jr.; Stratmann, R. E.; Burant, J. C.; Dapprich, S.; Millam, J. M.; Daniels, A. D.; Kudin, K. N.; Strain, M. C.; Farkas, O.; Tomasi, J.; Barone, V.; Cossi, M.; Cammi, R.; Mennucci, B.; Pomelli, C.; Adamo, C.; Clifford, S.; Ochterski, J.; Petersson, G. A.; Ayala, P. Y.; Cui, Q.; Morokuma, K.; Malick, D. K.; Rabuck, A. D.; Raghavachari, K.; Foresman, J. B.; Cioslowski, J.; Ortiz, J. V.; Stefanov, B. B.; Liu, G.; Liashenko, A.; Piskorz, P.; Komaromi, I.; Gomperts, R.; Martin, R. L.; Fox, D. J.; Keith, T.; Al-Laham, M. A.; Peng, C. Y.; Nanayakkara, A.; Gonzalez, C.; Challacombe, M.; Gill, P. M. W.; Johnson, B. G.; Chen, W.; Wong, M. W.; Andres, J. L.; Head-Gordon, M.; Replogle, E. S.; Pople, J. A. *Gaussian 98*, revision A.1x; Gaussian, Inc.: Pittsburgh, PA, 1998.
(29) Barone, M.; Cossi, B.; Mennucci, B.; Tomasi, J. *J. Chem. Phys*. **1997**, *107*, 3210.
(30) Riddik, J. A.; Bunger, W. B.; Sakano, T. K. *Organic Solvents*, 4th ed.; John Wiley and Sons: New York, 1987; Vol. II, p 75.
(31) Tomasi J.; Persico M. *Chem. Rev*. **1994**, *94*, 2027.
(32) Kendall, R. A.; Dunning, T. H., Jr.; Harrison, R. J. *J. Chem. Phys*. **1992**, *96*, 6796.

TABLE 1. MP2/AUG-cc-pVDZ Calculated Relative Energies, E_R (kcal/mol), of the Stable Neutral and Anionic Forms of AHA Considering the Molecule Isolated and in the Presence of Solvent[a]

	isolated molecule		PCM			
	E_R	μ	E_R	μ	$\Delta G_{s(MP2)}$	$\Delta G_{s(RHF)}$
AHA neutral						
(*Z*)-amidic ((*Z*)-A)	0.0[b]	3.779	0.0[c]	4.781	−9.4	−10.8
(*E*)-amidic ((*E*)-A)	1.6	3.537	0.4	4.578	−10.6	−12.4
(*Z*)-imidic ((*Z*)-I)	1.1	0.317	1.9	0.154	−8.6	−9.2
(*E*)-imidic ((*E*)-I)	5.4	0.056	5.0	0.074	−9.8	−10.7
AHA anions						
(*Z*)-Ia anion	0.0[d]	3.296	0.0[e]	4.466	−63.2	−66.4
(*E*)-Ia anion	13.0	4.421	6.8	6.051	−69.4	−71.8
(*E*)-Ib anion	28.4	5.413	22.9	7.495	−68.7	−72.2
(*Z*)-II anion	17.2	7.449	6.5	9.876	−74.0	−78.4
(*E*)-II anion	12.3	2.283	8.9	2.827	−66.6	−69.4

[a] Solvation free energies, $^{\Delta}G_s$, are given in kcal/mol. Dipole moments, μ, are given in Debyes. [b] $E_a = -283.673447$ au. [c] $E_b = -283.688362$ au. [d] $E_c = -283.121064$ au. [e] $E_d = -283.221794$ au.

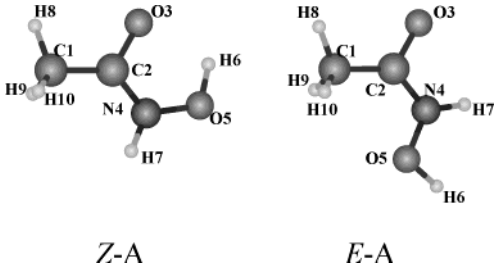

FIGURE 1. Neutral (*Z*)- and (*E*)-amidic forms of AHA.

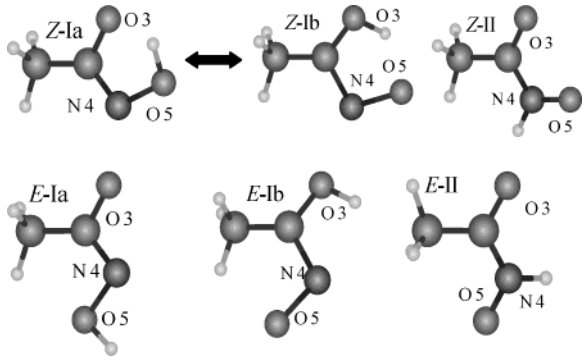

FIGURE 2. (*Z*)- and (*E*)-anions of AHA.

AHA presents different stable structures and shows amide−imide tautomerism; conformational analysis provides stable acidic forms. The internal rotation of the C−N bond that enables interconversion of the *Z*(cis) ⇌ *E*(trans) forms is hindered by barriers higher than 25 kcal/mol;[4] hence, the two forms can be treated as different species. The conformers generated by OH rotation and CH_3 torsion can be classified as (*Z*)-amidic, (*E*)-amidic, (*Z*)-imidic, and (*E*)-imidic forms. The (*Z*)- and (*E*)-isomers are assumed to coexist, giving rise to different deprotonation processes leading to formation of independent (*Z*)- and (*E*)-anions, respectively. Thus, the probability of the process involving the (*E*)-form must be taken into consideration for a proper interpretation of the mechanisms.

The minima for the MP2/cc-pVDZ and MP2/AUG-cc-pVDZ potential energy surfaces agree well. As expected, the diffuse functions modify slightly the relative energies of the neutral species; the energy change ranged from 2.8% (in the most stable (*E*)-imide tautomer) to 15.3% (in the most stable (*Z*)-imide tautomer). Table 1 lists the relative energies of the most stable neutral forms with respect to the (*Z*)-amide tautomer ($E = -283.673447$ au). The amide forms display nonplanar geometry (Figure 1), whereas the imide forms (not shown) adopt planar structures with formation of a C=N double bond. The intramolecular O3...H6−O5 H-bond and the steric hindrance of the methyl group cause the relative stabilities.[4] Another significant feature is the difference in dipole moment between the amide and imide forms, since the polar solvent effect is more significant on the amide structure; moreover, although the energy levels are separated by relatively high barriers, the (*Z*)-amide, the (*E*)-amide, and the (*Z*)-imide tautomers show similar stability. The (*E*)-amide tautomer lies only 1.6 kcal/mol above the (*Z*)-geometry; the most stable (*Z*)- and (*E*)-imide tautomers (termed (*Z*)-II imide tautomer and (*E*)-III imide tautomer) lie 1.1 and 5.4 kcal/mol above the (*Z*)-amide form, respectively.

To test the validity of the second-order Möller−Plesset approximation for determining relative energies, the calculations of the isolated molecule have been repeated with the MP4 method. With the exception of the (*E*)-amide, whose MP4 relative energy drops from 1.6 to 0.8 kcal/mol, there are not significant changes with respect to the data shown in Table 1.

Anion Forms. (*Z*)-AHA displays the three (*Z*)-Ia, (*Z*)-Ib, and (*Z*)-II anions (Figure 2), the most stable of them being (*Z*)-Ia. (*E*)-AHA gives rise to three less stable anions. In the case of Ib-type anions, (*E*)-Ib represents a conformer, whereas the geometry of (*Z*)-Ib is unstable, although a rotamer of (*Z*)-Ib may exist. In these structures, the remaining H atom is bonded to O5, O3, and N4, respectively; their MP2/AUG-cc-pVDZ relative energies are listed in Table 1. Extension of the basis set causes an energy change of some 45%, this feature indicating that calculations of the AHA anions require the use of basis sets containing diffuse orbitals.

The (*Z*)-Ia and (*Z*)-II anions arise from geometry optimization of the neutral (*Z*)-amide after elimination of one proton, either H7+ or H6+ (see Figure 3, A = (*Z*)-amide; I = (*Z*)-imide form II); in the amide tautomer, H6 is bound to O5, and H7 to N4. After elimination of H7+ (R1 process), optimization affords the most stable Ia anion ($E = -283.121064$ au). Loss of H6 (R2 process) gives rise to the (*Z*)-II anion ($E = -283.0936$ au). On the

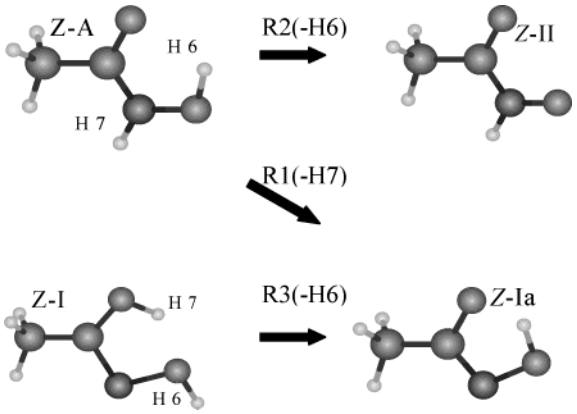

FIGURE 3. Deprotonation process of (*Z*)-AHA.

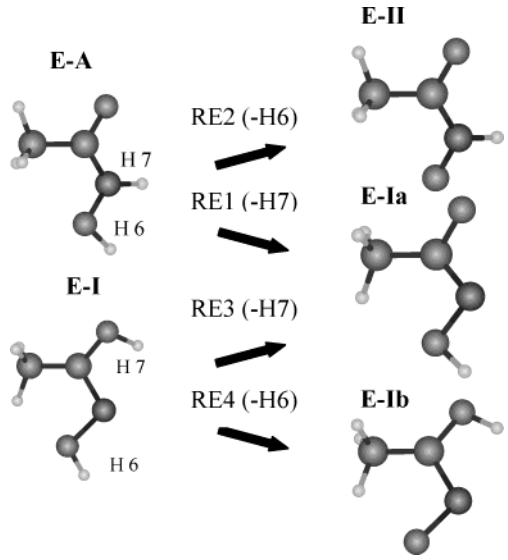

FIGURE 4. Deprotonation of (*E*)-AHA.

other hand, H7 is bound to O3 in the (*Z*)-imide tautomer; in this case, elimination of H6 (R3 process) produces the (*Z*)-Ia anion, and loss of H7+ gives one of the (*Z*)-Ia anion rotamers. The conformers generated by the OH and CH_3 internal rotations produce rotamers of the (*Z*)-Ia, (*Z*)-Ib, and (*Z*)-II anions. Loss of H atoms from the neutral (*E*)-forms gives rise to three different anions (Figure 4). After elimination of H6+ or H7+ (RE2 and RE1 processes), the (*E*)-amide tautomer can produce the most stable (*E*)-II anion ($E = -283.101532$ au) and (*E*)-Ia anion ($E = -283.100375$ au). The (*E*)-imide form can produce the (*E*)-Ia and (*E*)-Ib anions ($E = -283.075842$ au) after elimination of H7+ or H6+ (RE3 or RE4 processes).

The product of the R3 process is the (*Z*)-Ia anion rather than the (*Z*)-Ib form, since this was found to be unstable at the MP2 level. Figure 2 shows two (*Z*)-structures, (*Z*)-Ia and (*Z*)-Ib anions, connected by the interconversions O3···H6−O5 and O3−H6···O5 (see Figure 1). The stable (*Z*)-Ia anion has a planar structure, with the methyl group antieclipsed with respect to O3, and H6 connected to O5. The H-bond closes a cycle with a 2.5448 Å distance between the two oxygens. The O3···H6 equilibrium intramolecular H-bond distance was evaluated to be 1.8170 Å and the MP2/AUG-cc-pVDZ dipole moment to be 3.2959 D. However, (*E*)-Ia anion exhibits minimum

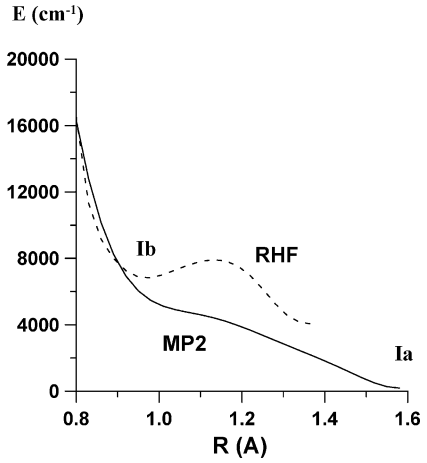

FIGURE 5. Energy change of the O3H6···O5O3···H6O5 interconversion as a function of the O3H6 bond distance.

energy conformations. Some rotamers of the (*Z*)-Ib anion shown in Figure 2 display some stability, although this anion, denoted as 4 A2 by Yazal and Pang,[33] is reported to be unstable with the Density Functional Theory.

There is no experimental evidence of the (*Z*)-Ib anion. The (*Z*)-Ia anion ↔ (*Z*)-Ib anion interconversion was simulated searching for the minimum energy path. Figure 5 plots the change in energy as a function of R (R = O3H6); the remaining coordinates were fully optimized for each selected structure. The (*Z*)-Ia anion ($R = 1.8170$ Å) represents the unique minimum of the MP2/AUG-cc-pVDZ path, although the gradient decreases in the region where the RHF curve (dashed line) shows a second minimum ($R = 0.97$ Å). RHF calculations led to two equilibrium structures separated by a transition state ($R_{TS} = 1.07$ Å). The stability of the (*Z*)-Ib anion decreases according to a correlation already observed.[2]

The two isomers of anion II, (*E*)- and *Z*, lie 12.3 and 17.2 kcal/mol above the (*Z*)-Ia anion (Table 1). The interconversion (*Z*)-II anion ↔ (*E*)-II anion requires that a potential barrier of 50.3 kcal/mol be overcome. In the (*Z*)-II anion, the methyl group is antieclipsed with respect to O3. The O3C2N4O5 frame is distorted to minimize the steric interactions of the two oxygens (O3O5 = 2.9295 Å). For instance, the O5N4C2 angle changed from 107.6° in the (*Z*)-Ia anion to 128.2° in the (*Z*)-II anion. In the (*E*)-II anion, the methyl group eclipses O3; the two oxygens are disengaged, but the charge distribution blocks the intramolecular H-bond stabilization. The Gibbs energy change of the interconversion (*Z*)-II anion ↔ (*E*)-II anion was evaluated to be −5.7 kcal/mol, a value that also decreases with temperature.

Solvent Effect. In ab initio calculations performed in solution, water was regarded as a continuous dielectric, characterized by a constant permittivity. The Polarizing Continuum Model (PCM) was used, implemented in the Gaussian 98 package.[29] Table 1 lists the relative energies (E_R) of the most stable anions and neutral forms calculated with MP2/PCM/AUG-cc-pVDZ; also listed are the solvation energies (ΔG_S(MP2)), defined as the difference between the MP2 energies of the isolated species and the corresponding values in solution and the solvation ener-

(33) El Yazal, J.; Pang, Y. P. *J. Chem. Phys.* **1999**, *103*, 8346.

TABLE 2. Thermodynamic Properties (kcal/mol) Corresponding to the Most Probable deprotonation Processes of AHA

	isolated molecule ($AH \rightleftharpoons A^- + H^+$)						PCM ($AH_s \rightleftharpoons A^-_s + H^+_s$)		
process	D_e	ΔH_{298}	$(T\Delta S)_{298}$	ΔG_{298}	ΔG_{308}	ΔG_{318}	ΔG_{298}	ΔG_{308}	ΔG_{318}
				(*Z*)-forms					
R1: amide ⇌ (*Z*)-Ia anion	338.3	338.9	6.9	332.0	331.7	331.4	170.7	170.4	170.1
R2: amide ⇌ (*Z*)-II anion	355.7	356.3	7.1	349.2	348.9	348.7	177.1	176.8	176.6
R3: imide ⇌ (*Z*)-Ia anion	337.3	337.9	7.0	330.9	330.6	330.4	168.8	168.5	168.3
				(*E*)-forms					
RE1: amide ⇌ (*Z*)-Ia anion	348.9	349.5	7.8	341.7	341.4	341.3	175.4	175.1	175.0
RE2: amide ⇌ (*Z*)-II anion	348.9	349.5	7.5	342.0	341.7	341.5	178.5	178.2	178.0
RE3: imide ⇌ (*Z*)-Ia anion	345.6	346.2	7.1	339.1	339.1	338.8	172.0	172.0	171.7
RE4: imide ⇌ (*Z*)-Ib anion	360.5	361.2	6.8	354.4	354.2	353.9	188.0	187.8	187.5

gies calculated at the RHF level (ΔG_s(RHF)). The two parameters ΔG_S(MP2) and ΔG_s(RHF) involve three nonelectrostatic contributions (cavitation, dispersion, and repulsion energies). As expected, the solvation effect on the neutral forms is negligible and somewhat larger for amides compared to imides. This effect, however, is important for the anions. The most stable (*Z*)-form is the (*Z*)-Ia anion ($E = -283.221794$ au), though the relative energy of the (*Z*)-II anion drops from 17.2 to 6.5 kcal/mol. For the (*E*)-forms, the solvent reverts the relative order of stability of (*E*)-II and (*E*)-Ia anions and favors (*E*)-N-deprotonation. The solvation free energies calculated at the Hartree−Fock level are shown in the last column of Table 1.

The presence of solvent increases all dipole moments. The dipole moments of the (*Z*)-Ia anion and the (*Z*)-II anion produce strong N- and O-deprotonation, respectively. A simple Mulliken analysis shows that the proximity of the two oxygens in the (*Z*)-II anion raises both the negative charge around the O5 and the electric moment. As expected, the largest solvation effect appears in the polar species (*Z*)-II, which becomes stabilized by 74.0 kcal/mol upon solvent addition. Solvation augments the Z−O-deprotonation probability.

Deprotonation Processes. The deprotonation site of AHA still is a matter of controversy, and generally a pronounced influence of the molecule environment is accepted.[34,35] For an isolated molecule (ideal gas model), the variation of the thermodynamic properties corresponding to the R1, R2, and R3 processes of the (*Z*)-forms (Figure 3) and the four RE1, RE2, RE3, and RE4 processes (Figure 4) at 298.15, 308.15, and 318.15 K are listed in Table 2 along with the properties calculated in the presence of solvent. For an isolated molecule, we consider the process $AH \rightleftharpoons A^- + H^+$ and treat the system as an ideal gas. The entropy values of the neutral and anionic species were taken from the Gaussian package output. In the presence of water, the Gibbs energies can be evaluated with the Born−Haber cycle:

$$\Delta G^{\text{solution}} = \Delta G^{\text{isolated molecule}} - \Delta G_s(\text{AH}) + \Delta G_s(\text{A}^-) + \Delta G_s(\text{H}^+) \quad (1)$$

where ΔG_s (AH), ΔG_s (A^-), and ΔG_s (H^+) are the solvation Gibbs energies of the acid species, anion, and proton, respectively (Table 1); ΔG_s (H^+) was calculated as ΔG_s (H_3O^+). Its value was calculated to be −107.5 kcal/mol with MP2/AUG-cc-pVDZ, far from the experimental value (−264.61 kcal/mol) employed in ref 36; $\Delta G^{\text{isolated molecule}}$ was evaluated with the gas ideal model and from the D_e dissociation energies ($\Delta H = D_e + p\Delta V$ and $\Delta G = \Delta H - T\Delta S$). The determination of D_e requires calculation of the total electronic energies and the zero-point energies performed in a harmonic analysis (ZPVE = 48.9 ((*Z*)-A), 49.0 ((*E*)-A), 48.9 ((*Z*)-I), 48.6 ((*E*)-I), 40.6 ((*Z*)-Ia), 40.0 ((*E*)-Ia), 39.6 ((*Z*)-Ib), 40.7 ((*Z*)-II), and 40.6 ((*E*)-II) (kcal/mol)). In the case of the solvent, we did not include the solvent effect on the vibrational analysis. In addition, the variation of the nonelectrostatic contributions to the solvation energy with the temperature has been neglected given the range of the temperature variation.

If the molecule is isolated, then the most likely process is N-deprotonation of the (*Z*)-amide, which produces (*Z*)-Ia anion (or formation of (*Z*)-Ia from the imide, in an equilibrium mixture of amide and imide). In this case, $\Delta G_{298.15}$ has been calculated to be 332.0 kcal/mol, in agreement with the experimental data of ref 18 measured in the gas phase (339.1 kcal/mol). This result supports previous ab initio calculations[21,23] and coincides with that determined for formohydroxamic acid.[2,24] The next probable processes are N and O deprotonation of the (*E*)-amide; from thermodynamic considerations, (*Z*)-O-deprotonation appears to be unlikely. Also, in solution the most probable process is the formation of the (*Z*)-Ia anion from the (*Z*)-amide and the (*E*)-Ia anion from the (*E*)-amide ($\Delta G_{298.15} = 170.7$ kcal/mol and $\Delta G_{298.15} = 175.4$ kcal/mol, respectively). However, (*Z*)-N-deprotonation is favored. The two processes, (*Z*)-O-deprotonation ($\Delta G_{298.15} = 177.1$ kcal/mol) and (*E*)-O-deprotonation ($\Delta G_{298.15} = 178.5$ kcal/mol), have a similar probability.

$\Delta G_{298.15}$ obtained from the experimental pK_{HA} value (see below) was smaller than the theoretical value in solution. The causes of the differences between experimental and calculated pK_{HA} values are discussed in ref 37.

Spectrophotometric Measurements: Acid Dissociation Constant. Within the ordinary pH range, AHA behaves as a simple monoprotic acid whose dissociation, represented by reaction 2,

$$HA \rightleftharpoons A^- + H^+ \quad (2)$$

(34) Eigen, M.; Kruse, W. Z. *Naturforsch. B* **1963**, *18*, 857.
(35) Diebler, H.; Secco, F.; Venturini, M. *J. Phys. Chem.* **1984**, *88*, 4229.
(36) Liptak, M. D.; Shields, G. S. *J. Am. Chem. Soc.* **2001**, *123*, 7314.
(37) Oliveira Silva, C.; Nascimento, M. A. C. *Adv. Chem. Phys.* **2002**, *123*, 423.

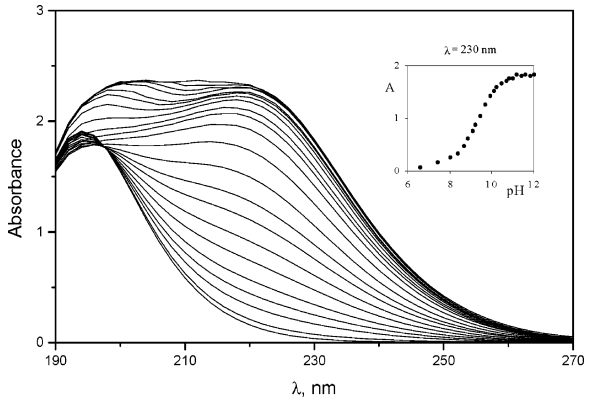

FIGURE 6. Set of spectral curves corresponding to ionization equilibrium of AHA. $T = 25$ °C, $I = 0.2$ M.

TABLE 3. pK_{HA} Values at Different Temperatures (I = 0.2 M)

T, °C	pK_{HA} (spectrophotometric)	pK_{HA} (potentiometric)
15	9.451 ± 0.003	9.45 ± 0.04
25	9.327 ± 0.003	9.30 ± 0.01
35	9.236 ± 0.004	9.24 ± 0.05
45	9.116 ± 0.002	9.11 ± 0.01
55	8.975 ± 0.003	8.93 ± 0.03
65		8.84 ± 0.06

was evaluated by UV titrations (Figure 6). The absorbance−pH data pairs were analyzed according to the following relationship:

$$A = \frac{A_{A^-} - A_{HA}}{1 + 10^{-m\mathrm{pH}+m\mathrm{p}K_{HA}}} + A_{HA} \qquad (3)$$

In eq 3, A represents the absorbance measured during titration. A_{A^-} and A_{HA} stand for the absorbances of the anion and the undissociated acid, respectively. K_{HA} represents the acid dissociation constant, and the parameter m is close to unity in aqueous solutions of pH 3−11.[38] An iterative minimization procedure allows the A_{A^-}, A_{HA}, and pK_{HA} values to be determined. Table 3 lists the pK_{HA} values at different temperatures and the ionic strength I = 0.2 M, which are in good agreement with literature values,[39] along with the $\Delta H° = 5.3$ kcal/mol and $\Delta S° = -23.5$ cal K^{-1} mol^{-1} values of reaction 2. Table 3 also lists the potentiometric results determined at the same temperatures.

Molar absorptivities, ϵ, of both the undissociated acid and the anion were determined at several wavelengths and at two different ionic strengths (Table 4); the observed independence of the anion ϵ values of the ionic strength reveals that dimerization does not ocurr in aqueous solution, a result confirmed by the ^{1}H NMR experiments described below.

^{1}H NMR Results. We are aware of only a single pK value published in the literature, the discussion being focused on which anion (O-anion or N-anion) is preferentially formed. Occurrence of the (*Z*)- and (*E*)-isomers of AHA in organic solvents has been reported, but not in aqueous solution. Brown et al.[6] reported cis−trans isomerism in DMSO-d_6 by ^{1}H, ^{13}C, and ^{15}N NMR measurements; NMR spectra have enabled clean assignment of the OH and NH protons of the (*Z*)-amide and (*E*)-amide isomers, yielding a 90:10 *Z*:*E* ratio in this solvent. On the other hand, experiments performed by Bagno et al.[14] in aqueous solution at pH 1 and pH 12 showed a single signal for AHA at each pH value. These authors provided three possible interpretations for this behavior: (a) the two forms undergo fast exchange, (b) the two forms display negligible difference in chemical shifts, or (c) only a single form is present in solution. They concluded that O-deprotonation is prevailing. However, in contrast with these authors, at room temperature, we found two ^{1}H NMR signals in water in the region characteristic of the methyl resonance, this feature suggesting that the neutral and anionic forms of AHA are present in aqueous solution as (*Z*)- and (*E*)-structures.

Figure 7 shows that both the neutral AHA form (pH = 5.20) and its anion (pH = 11.52) exhibit two signals. So far, there exists no evidence on which tautomer form, *Z* or *E* (amide or imide, respectively), is prevailing; however, for *N*-phenybenzohydroxamic acid, NMR measurements allowed the signal appearing upfield to be assigned to the (*Z*)-form. Moreover, kinetic results showed that the (*Z*)-tautomer is prevailing in water (92%).[11] Finally, the theoretical calculations reported in this work clearly indicate that the (*Z*)-form of AHA is prevailing both in the gas phase and in solution. On these grounds, it appears reasonable to assign the high-intensity and the low-intensity signals to the (*Z*)- and (*E*)-forms, respectively. Integration of the signals of Figure 7 indicates that the neutral (*Z*)-isomer amounts to 97% and the (*Z*)-anion amounts to 94% of the total dissolved AHA.

Figure 7 shows that the signals shifted to higher fields with increasing pH. Titration curves based on pH/chemical shifts are displayed in Figure 8a for the higher intensity signal ((*Z*)-AHA) and in Figure 8b for the lower intensity signal ((*E*)-AHA). Introduction of the δ_{AH}, δ_{A^-}, and δ chemical shifts corresponding to the acidic, basic, and intermediate forms, respectively, into eq 3 (δ instead of A) enables calculation of the K_Z and K_E microscopic dissociation constants of the (*Z*)- and (*E*)-tautomer forms. Since the NMR experiments were performed in deuterated water, to reliably compare a reaction in water with the same reaction in deuterium oxide, it was necessary to use the following conversion: actual pH of D_2O solution = apparent pH − γ. Given that the pK_{HA} value is around 9.0 (Table 3a), application of the Burton and Shiner treatment[40] leads to the ratio $K_{H_2O}/K_{D_2O} = 3.5$ for an acid species of similar strength and therefore to $\Delta\mathrm{p}K = \gamma = 0.54$. Hence, the values referring to an aqueous solution were p$K_E = 9.01 \pm 0.01$, and p$K_Z = 9.35 \pm 0.03$ at 25 °C. The difference in acid strength between the two isomers can be ascribed to the difference in the strength of the

(38) García, B.; Leal, J. M. *Collect. Czech. Chem. Commun.* **1987**, *52*, 299.

(39) (a) Wu, H. *J. Am. Chem. Soc.* **1977**, *99*, 1977. (b) Yamaki, R. T.; Paniago, E. B.; Carvalho, S.; Howarth, O. W.; Kam, W. *J. Chem. Soc., Dalton Trans.* **1997**, *24*, 4817. (c) Keeffe, J. R.; Jencks, W. P. *J. Am. Chem. Soc.* **1983**, *105*, 265. (d) Monzky, B.; Crumbliss, A. L. *J. Org. Chem.* **1980**, *45*, 4670. (e) Ryaboi, V. I.; Shenderovich, V. A.; Strizhev, E. F. Russ. *J. Phys. Chem.* **1980**, *54*, 730. (f) Ryaboi, V. I. *Zh. Fiz. Khim.* **1980**, *54*, 1279.

(40) Burton, C. A.; Shiner, V. J., Jr. *J. Am. Chem. Soc.* **1961**, *83*, 3207.

TABLE 4. Molar Absorptivities, ϵ, of Both the Protonated and Nonprotonated Species

HAH	ϵ_{209}	ϵ_{212}	ϵ_{215}	ϵ_{218}	ϵ_{220}	ϵ_{222}
$I = 1.00$ M	1318 ± 47	997 ± 36	687 ± 26	455 ± 22	338 ± 21	248 ± 20
$I = 0.25$ M	1462 ± 87	1046 ± 65	730 ± 51	499 ± 42	383 ± 39	292 ± 37
HA^-	ϵ_{220}	ϵ_{225}	ϵ_{230}	ϵ_{235}	ϵ_{240}	ϵ_{245}
$I = 1.00$ M	4139 ± 296	4470 ± 13	3924 ± 57	3017 ± 48	2105 ± 35	1378 ± 22
$I = 0.25$ M	4873 ± 140	4769 ± 99	4058 ± 38	3074 ± 16	2142 ± 8	1398 ± 7

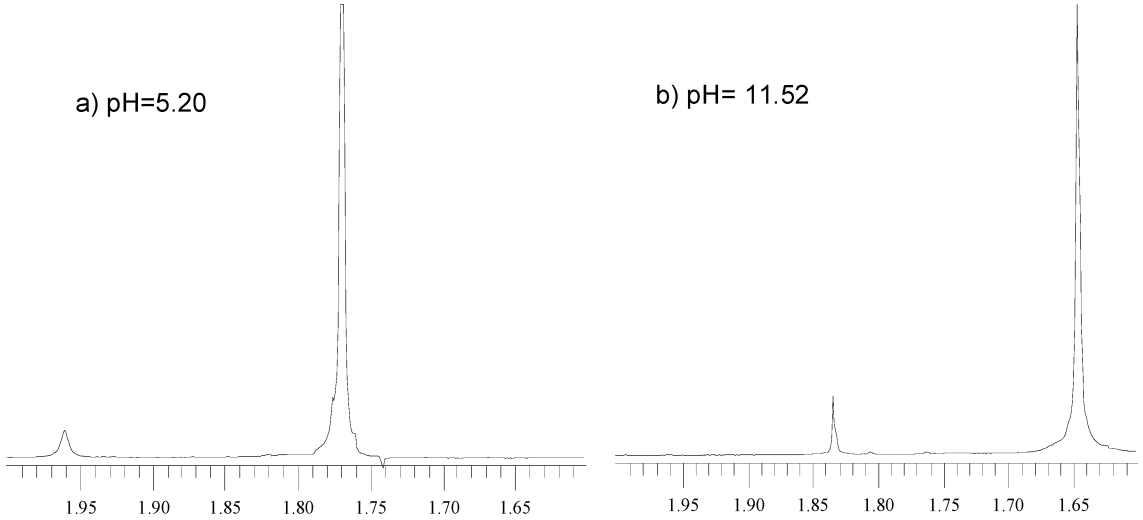

FIGURE 7. AHA signals in D_2O in the region characteristic of the methyl resonance. $T = 25$°C; (a) neutral forms, pH = 5.20; (b) anionic forms, pH = 11.52.

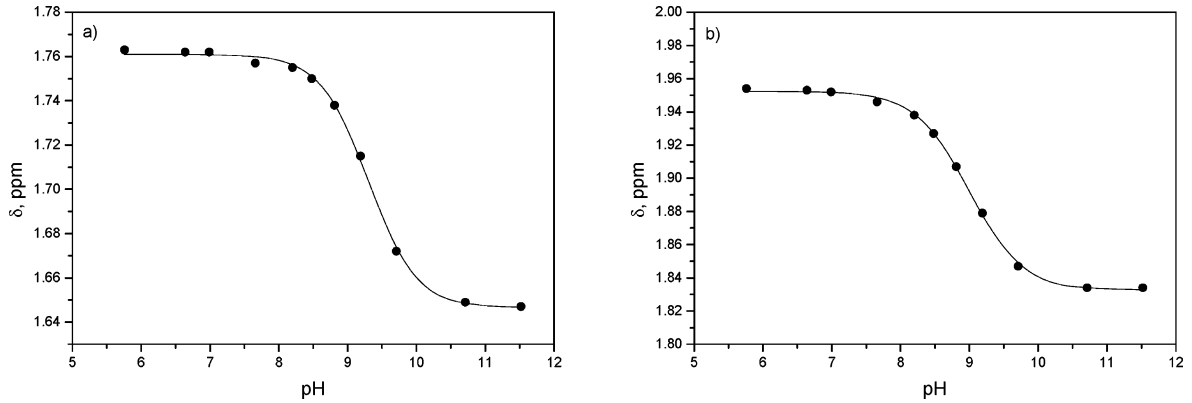

FIGURE 8. Variation of the chemical shift, δ, in D_2O as a function of pH. $T = 25$ °C; (a) high-intensity signal ((*Z*)-AHA); (b) low-intensity signal ((*E*)-AHA).

H-bond, either intramolecular or involving solvent; H-bonding stabilizes the proton of the (*Z*)-isomer, thus decreasing its acidity.

The distribution of AHA among different isomer species makes it difficult to decide which of the OH or NH forms preferentially dissociates. Figure 7 displays no signal ascribable to the H of AHA. Although the fast exchange with deuterium oxide prevents elucidation of which H of each isomer is more acidic and also discussion of whether the (*Z*)- and (*E*)-species behave as OH or NH acids in aqueous solution, the theoretical results listed in Table 2 show that in aqueous solution, the most likely processes correspond to N-deprotonation of both (*Z*)- and (*E*)-forms, namely, the R1, R3 and the RE1, RE3 processes shown in Figures 3 and 4, respectively.

As outlined in the Experimental Section, the temperature effect on the NMR signals in the 5−85 °C range (not shown) indicates that the signal of the (*E*)-isomer of the neutral species becomes broader starting from about 30 °C and overlaps with the baseline, whereas the two signals of the anions remain unchanged within the same temperature range; this feature points to a slow $Z^- - E^-$ and a fast $Z-E$ interconversion, relative to the NMR time scale. This result was confirmed by NOESY (one-dimensional) experiments (not shown) that reveal that the exchange between the anions is negligible at 25 °C (even at the high mixture time of 1 s) and modest at 80 °C (mixture time 0.4 s). This feature bears relation to the C=N double-bond character through which the isomeric interconversion occurs and reveals that the $Z-E$ conversion barrier is much larger for the anions than for the corresponding neutral molecules. Likewise, calculations in the gas phase showed that the $Z^- - E^-$ interconversion barrier amounts to about 10 kcal/mol above

SCHEME 1

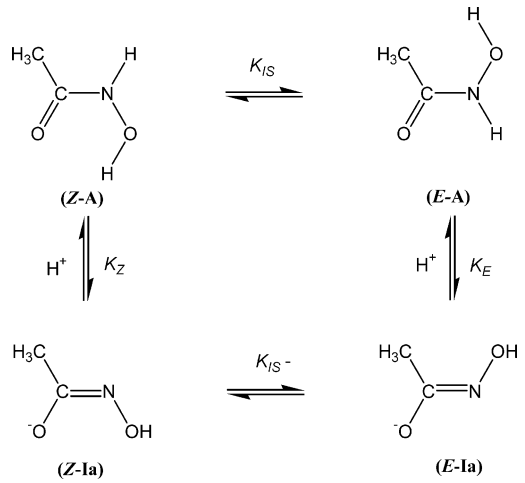

that of the $Z-E$ conversion. These results are consistent with a preference for N-deprotonation (R1 processes) over O-deprotonation (R2 processes), since the C−N bond in the N-anion exhibits a more extended double-bond character than in the O-anion (as inferred from the resonant forms), which hinders the rotation and $Z^- - E^-$ interconversion. Comparison of the dynamic NMR results for the neutral species with those of the anions supports the assumption that the C═N double-bond character is much less pronounced in the first case than in the second, which results in the prevalence of the neutral (CH_3 (O)C−NH(OH)) amide forms ((*Z*)-A and (*E*)-A) relative to the imide (CH_3 (OH)C═N(OH)) forms ((*Z*)-I and (*E*)-I). Therefore, the reaction in Scheme 1 is suggested.

According to Scheme 1, the macroscopic dissociation constant K_{HA} is given by eq 4.

$$K_{HA} = \frac{K_Z + K_E K_{IS}}{1 + K_{IS}} \qquad (4)$$

The NMR data of Figure 7 yield $K_{IS} = 3/97$ and $K_{IS^-} = 6/94$. Introduction of the K_{IS}, K_Z and K_E values into eq 4 yields $K_{HA} = 4.63 \times 10^{-10}$, in good agreement with the value determined at 25 °C by spectrophotometric and potentiometric measurements (Table 3). Finally, NMR experiments performed at different initial AHA concentrations demonstrated that chemical shifts were not influenced by the substrate concentration. Consistently, this feature supports the observation that in water, AHA is present only in the monomer form. It should be noted, for this purpose, that *N*-phenylbenzohydroxamic acid was found to dimerize in acetone but not in water.[11]

Conclusions

Ab initio calculations indicate that the (*Z*)- and (*E*)-isomers of acetohydroxamic acid present neutral and anionic stable forms. NMR spectroscopy also shows the existence of (*Z*)- and (*E*)-tautomers in aqueous solution, which so far had been only a theoretical hypothesis. Each tautomer has a different acidic strength. NMR spectroscopy allows the microscopic deprotonation constants of the (*Z*)-AHA and (*E*)-AHA forms to be evaluated, the combination of which provided an overall acid dissociation constant in good agreement with the value determined by spectrophotometric and potentiometric measurements. Comparison of the dynamic NMR and NOESY (one-dimensional) results for neutral species with those for anions reveals the occurrence of N-deprotonation in the (*Z*)-amide and (*E*)-amide in aqueous solution. The theoretical calculations agree with this conclusion.

Experimental Section

Chemicals. All chemicals used were analytical grade. Twice-distilled water was used to prepare the solutions and as a reaction medium as well. The ligand, acetohydroxamic acid (AHA), was of the highest purity commercially available (>99%). Stock solutions of AHA were kept in the dark at 4 °C. Perchloric acid and sodium perchlorate or potassium chloride were used to attain the desired medium acidity and ionic strength, respectively. NMR measurements were performed in D_2O (99.9%). The pH variation in NMR was attained with KOD (40% w/w, previously diluted with D_2O).

Methods. Hydrogen ion concentration of solutions below $[H^+] \leq 0.01$ M were determined by pH readings with a pH meter, calibrated with different buffer solutions within a pH range of 1.6−12.5. A combined glass electrode was used after replacing the usual KCl bridge with 3 M NaCl in order to avoid precipitation of $KClO_4$. The electrode was calibrated against sodium perchlorate−perchloric acid solutions of known concentration and ionic strength to directly give $-\log [H^+]$.

^{1}H NMR measurements were performed with a 400 MHz instrument at 9.4 T (operating at 399.941 MHz). The spectra were recorded at different temperatures between 5 and 85 °C using a spectral window of 15 ppm; acquisition times were 13.2 s. NOESY (one-dimensional) were determined with nonselective proton saturation under the following conditions: relaxation delay, 1.000 s; mixing between 0.2 and 1 s; acquisition time, 0.225 s. A Gauss apodization of 0.040 s and an FT size of 2048 × 2048 were used for data processing.

The absorption titrations were performed on a Diode Array spectrophotometer with a Peltier accesory to control the temperature. Experiments were performed at 15, 25, 35, 45, 55, and 65 °C. Increasing amounts of KOH were added by a microsyringe to a solution of AHA previously thermostated in the measuring cell. Fluctuations in temperature were within ±0.1 °C throughout. The medium acidity and ionic strength were kept constant at the desired values during each titration. The data were evaluated by nonlinear least-squares procedures.

Acknowledgment. Financial support by Ministerio de Ciencia y Tecnología, Spain, Projects AYA2002-02117 and BQU2002-01061, DGESIC PM98-0073, and Junta de Castilla y León BU26-02, Spain, are gratefully acknowledged. The authors thank Prof. J. Tomasi for useful suggestions and discussion.

Supporting Information Available: Theoretical results of the neutral and anionic forms. This material is available free of charge via the Internet at http://pubs.acs.org.

JO0341564